EXPERIMENTEL STUDY OF HEAT TRANSFER AUGMENTATION IN HEAT EXCHANGERS USING HELICAL WIRES.

K. A. ELADOULY, R. Y. SAKR, A. R. ELSHAMY AND K.M.ELSAZLY
Mech.Eng. Dept., Faculty of Eng. at Shoubra, Benha University, Cairo, Egypt.
108 Shoubra – Street, Cairo

ABSTRACT

Augmentation of heat transfer in the annulus side of tube in tube heat exchanger was investigated experimentally. The heat transfer as well as the flow characteristics was investigated. The test section used in the present study is a horizontal annular passage formed by two concentric tubes. The outer tube is made from PVC material and two different sizes of 47 and 72 mm inner diameters are used. The inner tube is a circular brass tube of 22 mm outer diameter and 6 mm thickness. A cylindrical heating element of 10 mm diameter is tightly inserted in the inner tube to simulate the hot stream side. The outer PVC tube is well insulated. Copper wires having diameters of 0.7, 1, and 1.5 mm are used as an artificial surface roughness enhancement elements. The copper wires are wrapped helically on the outer surface of the inner tube at four different pitches of 10, 20, 40 and 60 mm respectively. Several experimental runs were performed to show the effect of the helical wire diameter and pitch as well as the annulus diameter ratio. Also, all the experiments were carried out in the range of Reynolds of number, based on hydraulic diameter of the flow passage, from 7950 to 28900.

The results obtained from the present study showed that the heat transfer rates is increased with increasing the wire diameter and with decreasing the wire pitch. The highest enhancement ratio based on constant mass flow rate reached to a value of 2.04 compared with the smooth annulus case (without helical wire) at Re= 7950 with outer tube diameter of 47 mm. The increasing heat transfer rate due to the helical wires is accompanied with a considerable increase in the pressure drop and the friction factor. The highest average increase in friction factor is about 5.787 times the value of the smooth annulus and this took place at Re=21900 with helical wire having the pitch of 10mm and a diameter of 1.5 mm for outer tube diameter 72 mm. Also, the maximum net energy gain at the expense of increased pressure drop caused by helical wire insertions is about 30% and took place at wire diameter of 1 mm, wire pitch of 40 mm, Re=7950 and outer tube diameter of 47 mm. Also, some empirical correlations expressing the different heat transfer and friction parameters with the operating and design conditions were obtained.

LIST OF SYMBOLS

Symbol	Description	Unit
cp	specific heat of air at constant pressure	$KJ / Kg.C^{\circ}$
D_h	Hydraulic diameter	m
Di	inner tube diameter	m
Do	outer pipe diameter	m
dw	helical wire diameter	m
h	Overall heat transfer coefficient	$W/m^2.c$
L	length of tube	m
$\dot{m}$	mass flow rate of air flow	kg/s

P	pitch of helical wire	m
ΔP	pressure drop	Pa
q''	heat flux	w/m^2
R	resistance of heater	Ω
T	temperature	K^0
X	length of segment	m
V	Velocity	m/s

Greek Letters

μ	dynamic viscosity	m^2/s
ρ	density	kg/m^3

Dimensionless Parameters

ER	enhancement Ratio, $\overline{Nu}$ / Nu_0
f	friction factor
f_0	friction factor for smooth pipe
Nu_0	Nusselt number for smooth annulus
$\overline{Nu}$	average Nusslet number
PR_0	thermal hydraulic performance ratios
Pr	Prantdtl number
Re	Reynolds number

1- INTRODUCTION

Heat transfer enhancement is the process of improving the performance of a heat transfer system by increasing the heat transfer coefficient. In the past decades, heat transfer enhancement technology has been developed and widely applied to heat exchanger applications; for example, refrigeration, automotives, process industry, chemical industry, etc. To date large number of attempts have been made to reduce the size and costs of the heat exchangers. An increase in heat transfer coefficient generally leads to another advantage of reducing the temperature driving force, which increases the second law efficiency, and decreases entropy generation.

Bharadwaj et al. [1] determined experimentally the pressure drop and the heat transfer characteristics of water flow in a 75^o-start spirally grooved tube with and without twisted tape insert from laminar to fully turbulent ranges of Reynolds numbers. The grooves are clockwise with respect to the direction of flow. Compared to smooth tube, the heat transfer enhancement due to spiral grooves is further augmented by inserting twisted tapes having twist ratios of 10.15, 7.95 and 3.4. It is found that the direction of twist (clockwise and anticlockwise) influences the thermo-hydraulic characteristics. Constant pumping power comparisons with smooth tube characteristics showed that in spirally grooved tube with and without twisted tape, the heat transfer increases considerably in laminar and moderately in turbulent range of Reynolds number. However, for the bare tube and for spiral with anticlockwise twisted tape = 0.15, the reduction in heat transfer is noticed over a transition range of Reynolds numbers.

Ravigurarajan , A Dewan and Lieke [2,3,4] performed a comparative study of the thermal design correlations and performance comparison for the laminar and turbulent flow in helical-enhanced tubes and tube inserts. The variables considered in these investigations include the "design" parameters, namely, height, pitch, and helix angle of the rib, and the tube diameter; and "flow" variables such as the Reynolds number and the Prandtl number. The pressure drop and heat transfer correlations needed for the prediction of the performance of ribbed tubes can be developed using either an analogy approach or an empirical technique. These two methods are explained, along with the many correlations that had been developed based on them. The numerous studies pose a dilemma for the designer in selecting the most appropriate correlation.

Sivashanmugam and Suresh [5,6]studied experimentally the heat transfer and friction factor characteristics of turbulent and laminar flow through a circular tube fitted with full-length helical screw element of different twist ratio and helical screw inserts with spaces length of 100, 200, 300 and 400 mm with uniform heat flux. They observed that the heat transfer coefficient and friction factor increase with the twist ratio. They also found that the decrease in Nusselt for the helical twist with spaces length is within 10% for each subsequent 100 mm increase in spaces length and the friction factor for helical twist insert with spaces length of 100 mm is very much close to value of friction factor for full length helical twist for all Reynolds number and decrease by 5% for each 100 mm increment space length. The decrease in frication factor is nearly 40% for the twist ratio from 1.95 to 2.93 and decrease in the similar trend for each increase of twist ratio from 2.93 to 3.91 and from 3.91 to 4.89 for all Reynolds number range. They obtained empirical correlations for explaining the data and found that they fit the experimental data within ± 10 % and ± 20 % respectively for Nusselt number and friction factor.

Akhavan et al. [7] studied experimentally heat transfer and pressure drop characteristics of forced convective evaporation in horizontal tubes with coiled wire inserts. The test evaporator was electrically heated copper tube of 1200 mm length and 7.5 mm inside diameter. Helically wire coils with different wire diameters of 0.5, 0.7,1.0 and 1.5 mm and different coil pitches of 5, 8, 10 and 13 mm were made and used in full length of the test evaporator. For each inserted wire tube and also the plain tube, several test runs were carried out with different mass velocities and heat fluxes. From the analysis of the acquired data, it was found that the coiled wire inserts enhance the heat transfer coefficient but with a higher penalty due to the increasing of pressure drop, in comparison to that for the plain flow. An empirical correlation has been developed to predict the heat transfer coefficient during the evaporation inside a horizontal tube in the presence of a coiled wire insert.

Ebru [8] investigated experimentally the effect of different helical wires on the heat transfer, friction factors and the dimensionless exergy loss in a double concentric pipe heat exchanger. The heat transfer rates are found to be increased with decreasing the pitch and with increasing helical number of the helical wires used in the experiments.. Also it is found that the dimensionless exergy loss and NTU(number of heat transfer unit) increase with the increase of helical number and decreased with the increase of pitch. The increase was about 1.16 times that of the empty tube at the highest Reynolds number for helical wire having the pitch of 9 mm and the helical number of 137.

Garimella et al. [9,10] investigated experimentally the enhancement heat transfer in fluted tube annuli for the Reynolds number range $700 < Re < 40000$ used 14 fluted and

the effect of enhancement heat transfer on friction factor by using spirally fluted annuli over all three flow regimes (laminar, transition and turbulent). The study focused on the annulus side and the results serve as the basis for the understanding of heat transfer in spirally fluted annuli. The effects of geometry and flow related variables had modeled. They found that in low Re number range, using fluted inner tubes in an annulus causes increase in Nusselt numbers between 4 and 20 times higher than the corresponding smooth-annulus due to induced swirl flow and for turbulent flow, the enhancement is between 1.1 and 4.0 and the fluted annuls Nusselt number increases with an increase in flute depth, and with a decrease in flute pitch and annulus radius ratio.

They also found that the friction factor increases over smooth annulus values were typically between 1.1 and 2.0 for laminar flow, and up to 10 for turbulent flow and the annulus radius ratio is an important parameter in determining the fluted annulus friction factor.

Alberto et al. [11,12] studied experimentally enhancement heat transfer with wire coil inserts in laminar-transition and turbulent flow by using water and water-propylene glycol mixtures at different temperatures, a wide range of flow conditions corresponding to variation of Reynolds numbers from 80 to 90000. General correlations had been proposed for Fanning friction factor and Nusselt number as functions of wire geometry and flow conditions. In laminar flow, results show that wire coils behave mainly as a smooth tube. Transition to turbulent flow takes place at low Reynolds numbers (Re=700) and in a gradual way. Wire coils have a predictable behaviors within the transition region since they show continuous curves of friction factor and Nusselt number, which involves a considerable advantage over other enhancement techniques. In turbulent flow, wire coils cause a high pressure drop increase which depends mainly on pitch to wire-diameter ratio.

Eiamsa and Promvonge. [13,14,15] investigated experimentally the enhancements of heat transfer characteristics in a uniform heat flux circular tube fitted with conical nozzles and V-nozzle inserts. Three different pitch ratios of conical-nozzle arrangements in the test tube are introduced with pitch ratios of 2.0, 4.0 and 7.0 in each run. They found that the heat transfer in the circular tube could be enhanced considerably by fitting it with conical-nozzle inserts and the value of the Nusselt number increases in a range of 236 – 278 % over that of the plain tube for the conical-nozzle inserts However, the increase in pressure drop is much higher than the increase in Nusselt number at the same Reynolds number. The Nusselt number increases with reduction of the pitch ratio and the increase of Reynolds number. The maximum heat transfer rates obtained from using the conical nozzles with pitch ratios of 2.0

Saha, Dutta et al. [16,17] had been studied experimentally the heat transfer and the pressure drop characteristics in a circular tube fitted with twisted tapes laminar swirl flow of a large Prandtl number ($205 < Pr < 518$). Viscous fluid was considered. The swirl was generated by short length twisted-tape inserts. The reduction in Nusselt number for short–length twisted-tape is much less than the reduction in friction factor compared to full-length twisted-tape for tighter twists (twist ratio <5). On the basis of constant pumping power and constant heat duty, short length twisted-tapes (up to 33 percent length of the tube) is found to perform better than the full-length twisted-tapes.

Shou et al.[18] studied experimentally the turbulent heat transfer and the flow characteristics in a horizontal circular tube with strip-tape inserts. Friction factor data and

temperature measurements were used to understand the underlying physical phenomena responsible for the heat transfer enhancement for $6500 \leq Re \leq 19500$. They noticed that the thermal entrance length and buoyancy effects becomes smaller for tubes with inserts and the heat transfer enhancement of this tubes is about four to two times that of bare tubes for Re = 6500 to 19500. Also, they were evaluated overall performance based on constant pumping power and constant heat duty. Both show that the tubes with inserts were beneficial as far as economics was concerned

Garcia et al [19] carried out experimentally an analysis of the flow mechanism in tubes with wire coils using hydrogen bubble visualization and particle image velocity metry techniques. They found that shorted-pitch wire coils cause the appearance of a separated flow at Reynolds numbers closer to 400. This recirculation together with the azimuthally velocity component produces a helical flow which ascends along the wire coil body. In the wire with the longer pitch, a flow separation does not take place.

Leonard et al. [20] investigated experimentally the effect of internal aluminum fins with a star-shape cross-section on the heat transfer enhancement and pressure drop in a counter flow heat exchanger. A concentric-tube heat exchanger was used with water as a working fluid. They found that the overall heat transfer coefficient in a concentric-tube heat exchanger was enhanced with a star-shape fin insert by as much as 51% at a constant pumping power.

From the previous literature, it is noticed that there is a shortage for the heat transfer enhancement in the annulus side of the double pipe heat exchanger. So, the aim of this study to investigate experimentally the effect of wrapping helical wires on enhancement heat transfer.

2- EXPERIMENTAL SETUP AND CONDITIONS

2-1 Experimental Setup

The experimental apparatus used in the present study is shown in Fig. (1). It consists mainly of : air supply unit, test section and different measuring instruments. The test section is a horizontal annular passage formed by two concentric tubes. The outer tube is circular PVC- tubes size of 47 mm and 72 inner diameters. The inner tube is a circular brass tube of 22 mm outer diameter and 6 mm thickness. To ensure the concentricity of the two pipes, the outer pipes was fitted with three bolts of 6mm diameter and two wooden rings with the same dimensions of the annular radii are manufactured and inserted partially into the annulus to adjust the concentricity. Heat is transferred mainly from the outer surface of the inner tube while outer PVC-is tubes well insulated. The heater used is ready-made heater of total electrical resistance 24.2 ohm with a diameter of 10 mm and length of 2000 mm which is fitted into the brass tube. Circular copper wires (helical elements) are used as surface roughness enhancement elements with diameters of 0.7,1 and 1.5mm. The copper wires are fluted over the inner tube to form a helical elements on the inner tube with different pitches.

So, experiments on the 24 geometric configurations are performed for eight values of Reynolds number.

2-2 Experimental Conditions

Geometrical results are presented in terms of the helical wire diameter (dw), the helical wire pitch (P), inner tube diameter (Di), and outer tube diameter (Do). The helical wire diameter to inner diameter ratios dw/Di =0.032, 0.045 and 0.068. The helical wire pitch to inner diameter ratios P/Di = 0.45, 0.9, 1.8, 2.7. The outer to inner diameter ratios for the annulus Do/Di = 2.14 and 3.27; and all the geometrical results are carried out at different operating Reynolds number (based on the hydraulic diameter D_h and bulk mean velocity), ranged from 7950 to 30000.

2-3 Instrumentation

The air-flow rate was obtained by a calibrated orifice-meter. Pressure taps were located on the tube surface to measure pressure drop along the test section. The pressure drop across the orifice-meter and the test section were measured by U-tube manometer. The surface temperatures of inner tube were measured at several axial positions using calibrated Chromel-Alumel K-type thermocouples whose wire diameter is 0.5 mm. The thermocouples were fixed to the outer surface of the inner tube. Thermocouples, which could be traversed vertically, are used to measure the bulk mean air temperature entering and leaving the test section. Bulk temperatures at all other thermocouple locations were calculated from the energy balance. Also, the electric power input to the heater can be controlled by voltage regulator, which provided controllable constant heat flux.

3-DATA REDUCTION AND UNCERTAINTY ANALYSIS

The heat input to an element of the test section via the main heater segments can be distributed into the following items:

1- Heat transferred by convection to the air flow in the tube (the useful part).
2- Heat transferred by radiation to the air flow.
3- Heat lost by radial conduction through the insulation layers.

Moreover, a previous work which carried out by Abdel Moneim [21] in the same temperature level has concluded that, the heat lost by axial conduction, by radial conduction through the insulation layers and by radiation from the two ends of the test tube is very small and can be neglected. Therefore, the total heat input to the main heater segments was considered to be converted to the air flow.

3-1 Calculation of the friction factor

The mass flow rate was set at a desired value. The friction factor (f) of the periodically fully developed flow was calculated from the pressure drop along the annuals tube as:

$$\overline{f} = \frac{\Delta P D_h}{2\rho V^2 L} \tag{1}$$

The maximum uncertainty of the friction factor was estimated as 8.59%.

The electrical power generated from the main heater, q, at the steady state was determined from the measured voltage, V, and the measured main heater resistance, R, as:

$$q = \frac{V^2 \cos\phi}{R} \tag{2}$$

The power factor, cos Φ, was found 0.98 for the present resistive load (heater).

When the steady state was achieved, the thermocouples reading were recorded. The local heat transfer coefficient, h_x, and corresponding local Nusselt number (Nu_x) were calculated, respectively, as follows:

$$h_x = \frac{q}{A_s\left(T_{s,x} - T_{m,x}\right)} \tag{3}$$

$$Nu_x = \frac{h_x D_h}{k} \tag{4}$$

Where,

h_x is local heat transfer coefficient (W/m.C°), Ts,x is tube wall temperature (C°), Tm,x is air bulk temperature (C°) and k is the thermal conductivity (w/m^2.C°).The uncertainty of 1.54% was found in calculating the local Nusselt number(Nu_x).

The average heat transfer coefficient and the corresponding average Nusselt number were calculated at different flow velocities as:

$$\bar{h} = \frac{1}{L}\int_0^L h_j(x)dx \tag{5}$$

$\bar{h}$: Average heat transfer coefficient, (W/mc°).

L : Total length of the test section, (m).

and the average Nusselt number is calculated, from the following equation:

$$\overline{Nu} = \frac{\bar{h}D_h}{k} \tag{6}$$

The average Nusselt numbers of the present study are normalized by the Nusselt number for fully developed turbulent flow in smooth annulus to obtained the enhancement ratio

$$ER = \frac{\overline{Nu}}{\overline{Nu_0}} \tag{7}$$

The friction factor of helical annulus also is normalized by the friction factor for fully developed turbulent flow in smooth annulus .

The thermal hydraulic performance analysis is important for the evaluation of the net energy gain to determine if the method employed to increase the heat transfer is effective from energy point of view. The performance ratio is defined using the Nusselt numbers and friction factor for a smooth pipe and pipe wrapped with helical wire as follows:

$$PR_O = \frac{Nu/Nu_0}{\left(f/f_0\right)^{1/3}} \tag{8}$$

4- RESULTS AND DISCUTION

4-1 Smooth Annulus Results:

To check the perfect installation of the experimental set up, the correction of the experimental procedures, the method of calculations and the accuracy of measuring instruments. Several experimental runs were carried out for the smooth pipe (without using wires).Figure (2) illustrates the present experimental results compared with the previous published results of Kays and Leung, Dittus and Boelter [22**].**

Figure (3) depicts the experimental results for the friction factor compared with Blasius equation [23]**.** From these figures, it is observed that the present experimental results and those obtained from the previous studies are in good agreements so, the experimental runs that investigate the effect of helical wires geometry as roughness elements as well as Reynolds number are ready to be performed on the test rig.

4-2 Friction Annulus Results

4-2-1 Local Nusselt number

The influence of helical wire wrapped around the inner pipe on the local Nusselt number for the entrance and the fully developed regions inside the test section under uniform heat flux conditions are shown in figures (4) to (7) and the results of the local Nusselt number along the test section length for helical wire wrapped around the inner pipe in terms of X/D_h for the studied range of Reynolds number is compared with that for steady-state conditions with smooth annulus.

4-2-1-1 Effect of Reynolds number

Figure (4) shows the variation of the local Nusselt number along length of the inner pipe of the test section. This is for wire to inner pipe diameter ratio (dw/Di) =0.07 and outer to inner pipe diameter ratio (Do/Di)=3.27 for different values of Reynolds numbers. The figure illustrated that as Reynolds number increases the local Nusselt number increases. Also a sharp decrease for the local Nusselt number observed up to X/D_h=8 corresponding to the flow in the entrance region in the annulus and the lower is the Reynolds number the longer in the entrance region in the annulus .

Also, the figure illustrated that at distance X/D_h= 74 the effect of Reynolds is dimensioned, due to heat loss in the axial direction.

4-2-1-2 Effect of pitch

The effect of wire pitch on the local Nusselt number variation along the inner pipe length for Re=10100, dw/Di=0.032 and Do/Di=3.27 in is illustrated in Fig.(5). The figure shows that the local Nusselt number increase with the decrease of pitch to inner diameter ratio (P/Di).

4-2-1-3 Effect of friction wire diameter

The effect of wire to inner diameter ratio on the local Nusselt number for P/Di=0.91, Re=17300, and Do/Di=3.27 is illustrated in Fig.(6). The figure depicts that as the wire to inner diameter ratio increases the local Nussult number increases. This may be due to higher turbulence level generated for layer wire to inner diameter ratio.

4-2-2 Average Nusselt number

4-2-2-1 Effect of Reynolds number

The average Nusselt number with wire pitch at dw/Di=0.045 and Do/Di=2.14 for different Reynolds number is depicted in Fig.(7). It is noticed that as Reynolds number increases the average Nusselt number increases and as stated before, the increases of wire pitch leads to decrease in the average Nusselt number. The same behavior is observed for outer to inner diameter ratio Do/Di=3.27 in Fig.(8)

4-2-2-2 Effect of friction wire pitch

The variation of the Nusselt number with Reynolds number for different wire pitch at dw/Di=0.068 and Do/Di=2.14 is illustrated in Fig.(9). It is observed from the figure that increase of pitch to diameter ratio decreases the average Nusselt number . This may be explained as the wire pitch increases, the turbulence level decreases and the heat transfer ratio decreases also. The same behavior is observed for dw/Di=0.068, and Do/Di=3.27 is illustrated in Fig.(10).

4-2-2-3 Effect of friction wire diameter

The variation of average Nusselt number with Reynolds number at P/Di=0.91 and Do/Di=2.14 for different wire diameter is illustrated in Fig.(11). It is clear from figure that, as the wire diameter increases the average Nusselt number increases and this may be due to higher turbulence level is generated at higher values of wire diameter and consequently, more heat is transfer from the inner heater to the air stream. The same behavior is noticed for P/Di=0.91 and Do/Di=3.27 for Fig.(12).

4-2-2-4 Effect of diameter ratio

The variation of the average Nusselt number with Reynolds number at P/Di=0.45 and dw/Di=0.068 for different diameter ratio is shown in Fig.(13). The increase of the diameter ratio leads to increase in the average Nusselt.

From the previous results, the average Nusselt number is correlated as a function of Reynolds number, wire pitch to inner pipe diameter ratio, and wire diameter to inner pipe diameter ratio as follow

$$Nu = 10.393 \times (\mathrm{Re})^{0.3453} \times \left(\frac{dw}{Di}\right)^{0.62156} \times \left(\frac{p}{Di}\right)^{0.00394} \times \left(\frac{D0}{Di}\right)^{1.524}$$

where

$$7900 \le \mathrm{Re} \le 29000,\ 0.03 \le \frac{dw}{Di} \le 0.07,\ 0.4 \le \frac{p}{Di} \le 2.8,\ 2.2 \le \frac{Do}{Di} \le 3.3$$

with max. deviation of 12.8%.

4-2-3 Average friction factor

4-2-3-1 Effect of Reynolds number

The friction factor results with wire pitch at dw/Di=0.045 and Do/Di=2.14 for different Reynolds number is depicted in Fig.(14). It is noticed that as Reynolds number increases the friction factor decreases and increases of wire pitch leads to decrease in the friction factor. The same behavior is observed for outer to inner diameter ratio Do/Di=3.27 in Fig.(15).

4-2-3-2 Effect of friction wire pitch

The variation of the friction factor with Reynolds number for different wire pitch at dw/Di =0.068 and Do/Di =2.14 is illustrated in Fig.(16). It is observed from the figure that increase of pitch to diameter ratio decreases the friction factor. This may be explained as the wire pitch increases, the turbulence level decreases and the heat transfer ratio decreases also. The same behavior is observed for dw/Di =0.068, and Do/Di =3.27 is illustrated in Fig.(17).

4-2-3-3 Effect of friction wire diameter

The variation of friction factor with Reynolds number at P/Di=0.91 and Do/Di =2.14 for different wire diameter is illustrated in Fig.(18). It is clear from figure that, as the wire diameter increases the friction factor increases and this may be due to higher turbulence level is generated at higher values of wire diameter. The same behavior is noticed for P/Di=0.91 and Do/Di=3.27 for Fig.(19).

4-2-3-4 Effect of diameter ratio

The variation of the friction factor with Reynolds number at P/Di=0.45 and dw/Di=0.068 for different diameter ratio is shown in Fig.(20). The increase of the diameter ratio leads to increase in the friction factor .

From the previous results, the friction factor is correlated as a function of Reynolds number, wire pitch to inner pipe diameter ratio, and wire diameter to inner pipe diameter ratio as follow

$$f = 20.43 \times \mathrm{Re}^{-0.6416} \times \left(\frac{dw}{Di}\right)^{1.099} \times \left(\frac{p}{Di}\right)^{-0.3106} \times \left(\frac{Do}{Di}\right)^{3.672}$$

where

$$7900 \le \mathrm{Re} \le 29000\,,\ 0.03 \le \frac{dw}{Di} \le 0.07\,,\ 0.4 \le \frac{p}{Di} \le 2.8\,, 2.2 \le \frac{Do}{Di} \le 3.3$$

with max. deviation of 10.8%.

4-3 Constant Mass Flow Rate Enhancement Ratio

When the friction pumping power is not an issue, the enhancement ratio will depends only on the heat transfer enhancement. The enhancement ratio in this case can be defined as the ratio between the average Nusselt number in case of use the friction wire to the average Nusselt in smooth case .

$$\mathrm{ER} = \frac{\overline{Nu}}{\overline{Nu_0}}$$

4-3-1 Effect of Reynolds number

Figure (21) illustrated the effect of Reynolds number on the enhancement ratio ER, at dw/Di=0.07 and Do/Di=2.14. It is noticed from the figure that as the wire pitch increases the enhancement ratio decreases. Also, the enhancement ratio decreases with increase of Reynolds number. The maximum augmentation of the heat transfer process take place at Re=7950 and P/Di=0.45 and the enhancement ratio reaches to 153.93%.

Figure (22) illustrated the effect of Reynolds number on the enhancement ratio ER, at dw/Di=0.07 and Do/Di=3.27. It is noticed from the figure that as the wire pitch increases the enhancement ratio decreases. Also, the enhancement ratio decreases with increase of Reynolds number. The maximum augmentation of the heat transfer process take place at Re=10100 and P/Di=0.45 and the enhancement ratio reaches to 139.44%.

4-3-2 Effect of wire pitch

Figure (23) illustrated the effect of wire pitch on the enhancement ratio ER, at dw/Di=0.07 and Do/Di=2.14. It is noticed from the figure that as the wire pitch increases the enhancement ratio decreases. Also, the enhancement ratio decreases with increase of Reynolds number. The maximum augmentation of the heat transfer process take place at Re=7930 and P/Di=0.4 and the enhancement ratio reaches to 204.36%.

Figure (24) illustrated the effect of wire pitch on the enhancement ratio ER, at dw/Di=0.07 and Do/Di=3.27. It is noticed from the figure that as the wire pitch increases the enhancement ratio decreases. Also, the enhancement ratio decreases with increase of Reynolds number. The maximum augmentation of the heat transfer process take place at Re=10100 and P/Di=0.45 and the enhancement ratio reaches to 180.27%.

4-3-3 Effect of friction wire diameter

Figure (25) illustrated the effect of friction wire diameter on the enhancement ratio ER, at P/Di=0.45 and Do/Di=2.14. It is noticed from the figure that as the wire diameter increases the enhancement ratio increases. Also, the enhancement ratio decreases with increase of Reynolds number. The maximum augmentation of the heat transfer process take place at Re=7930 and P/Di=0.45 and the enhancement ratio reaches to 204.36%.

Figure (26) illustrated the effect of friction wire diameter on the enhancement ratio ER, at P/Di=0.45 and Do/Di=3.27. It is noticed from the figure that as the wire diameter increases the enhancement ratio increases. Also, the enhancement ratio decreases with increase of Reynolds number. The maximum augmentation of the heat transfer process take place at Re=10100 and dw/Di=0.07 and the enhancement ratio reaches to 180.27%.

4-3-4 Effect of diameter ratio

Effect of annuals diameter ratio on the enhancement ratio at P/Di=0.45 and dw/Di=0.068is illustrated in Fig.(27). From the figure, it is depicted that as the diameter ratio increases the enhancement ratio decreases.

From the previous results, the enhancement ratio is correlated as a function of Reynolds number, wire pitch to inner pipe diameter ratio, and wire diameter to inner pipe diameter ratio as follow

$$ER = 53.35(\mathrm{Re})^{-0.133}\left(\frac{dw}{Di}\right)^{0.621}\left(P/Di\right)^{0.00394}\left(\frac{Do}{Di}\right)^{-0.4382}$$

where

$$7900 \le \mathrm{Re} \le 29000,\ 0.03 \le \frac{dw}{Di} \le 0.07, 0.4 \le \frac{p}{Di} \le 2.8, 2.2 \le \frac{Do}{Di} \le 3.3$$

with max. deviation of 4.92

4-4 Friction Factor Ratio

4-4-1 Effect of Reynolds number

Figure (28) illustrated the effect of Reynolds number on the friction factor ratio, at dw/Di=0.07 and Do/Di=2.14. It is noticed from the figure that as the wire pitch increases

the friction ratio decreases. Also, the friction ratio increases with increase of Reynolds number. The maximum friction factor ratio take place at Re=24350 and P/Di=0.45 and the friction ratio reaches to 446.33%.

Figure (29) illustrated the effect of Reynolds number on the friction factor ratio, at dw/Di=0.05 and Do/Di=3.27. It is noticed from the figure that as the wire pitch increases friction ratio decreases. Also, friction ratio increases with increase of Reynolds number. The maximum friction ratio process take place at Re=21900 and P/Di=0.45 and the friction ratio reaches to 346.4%.

4-4-2 Effect of friction wire pitch

Figure (30) illustrated the effect of wire pitch on the friction factor ratio, at dw/Di=0.068 and Do/Di=2.14. It is noticed from the figure that as the wire pitch increases the friction factor ratio decreases. The maximum friction factor ratio take place at Re=24350 and P/Di=0.4 and the friction factor ratio reaches to 451.24%.

Figure (31) illustrated the effect of wire pitch on the friction factor ratio, at dw/Di=0.07 and Do/Di=3.27. It is noticed from the figure that as the wire pitch increases friction factor ratio decreases. Also, the friction factor ratio increases with increase of Reynolds number. The friction factor ratio take place at Re=21900 and P/Di=0.4 and the friction factor ratio reaches to 586.88%.

4-4-3 Effect of friction wire diameter

Figure (32) illustrated the effect of wire diameter on the friction factor ratio, at P/Di=0.45 and Do/Di=2.14. It is noticed from the figure that the variation in friction factor ratio is almost negligible with Reynolds number and increasing in wire diameter increase value the friction factor ratio. The friction factor ratio take place at Re=28920 and dw/Di=0.068 and reaches 462.6%.

Figure (33) illustrated the effect of wire diameter on the friction factor ratio, at P/Di=0.45 and Do/Di=3.27. It is noticed from the figure that the variation in friction factor ratio with Reynolds number is clearly at dw/Di=0.068, increasing Reynolds number increasing friction factor ratio Also, increasing in wire diameter increase value the friction factor ratio. The friction factor ratio take the maximum values at Re=21900 and dw/Di=0.068 and reaches to 586.88%.

4-4-4 Effect of diameter ratio

Effect of annuals diameter ratio on the friction factor ratio at P/Di=0.45 and dw/Di=0.068 is illustrated in Fig.(34). From the figure, it is depicted that variation of friction factor ratio is clearly appear at D0/Di=3.27 and at high Reynolds number, increasing the radius ratio increasing friction factor ratio. The maximum values of friction factor ratio=586.88 at Re=24450 and D0/Di=3.27 at P/Di=0.45 and dw/Di=0.068. From the previous results, the friction factor ratio is correlated as a function of Reynolds number, wire pitch to inner pipe diameter ratio, and wire diameter to inner pipe diameter ratio as follow

$$f/f_0 = 36.4022(\mathrm{Re})^{0.0694}\left(\frac{dw}{Di}\right)^{1.099}\left(\frac{p}{Di}\right)^{-0.3106}\left(\frac{Do}{Di}\right)^{0.0058}$$

where

$$7900 \le \mathrm{Re} \le 29000,\ 0.03 \le \frac{d_w}{Di} \le 0.07,\ 0.4 \le \frac{P}{Di} \le 2.8 \text{ and } 2.2 \le \frac{Do}{Di} \le 3.3$$

with max. deviation of 7.9%

4-5 Constant Pumping Power Enhancement Ratio

4-5-1 Effect of Reynolds number

Figure (35) illustrates the effect of Reynolds number on the performance ratio (PR_0) at dw/Di=0.068 and Do/Di=2.14. It is noticed from the figure that as the Reynolds number increases the performance ratio decrease. The maximum performance ratio based on the net energy is obtained at Re=7950, P/Di=1.8 and dw/Di=0.068 and have a value of 9%. For the larger value of Do/Di=3.27 the same behavior of the performance ratio with Reynolds number is observed in Figure (36). The maximum value of the performance ratio is obtained at similar P/Di = 1.8 For Re=10100, and dw/Di=0.068, the performance ratio reached at maximum values 0.5%.

4-5-2 Effect of friction wire pitch

Figure (37) showed the effect of wire pitch on the performance ratio (PR_0), at dw/Di=0.045 and Do/Di=2.14. It is noticed from the figure the maximum performance ratio =30% at P/Di=1.8 and dw/Di=0.045.

Figure (38) showed the effect of wire pitch on the performance ratio, at dw/Di=0.045 and Do/Di=3.27. It is noticed from the figure the maximum performance ratio =28% at P/Di=2.4.

4-5-3 Effect of friction wire diameter

Figure (39) illustrated the effect of wire diameter on the performance ratio (PR_0), at P/Di=0.45 and P/Di=2.14. It is noticed from the figure that the maximum performance ratio is 28% at dw/Di=0.068 and Re=7950.

Figure (40) illustrated the effect of wire diameter on the performance ratio (PR_0), at P/Di=0.45 and Do/Di=3.27. It is noticed from the figure that the maximum performance ratio is 22% at dw/Di=0.068 and Re=10100

6- Conclusions

1- The enhancement ratio (ER) decrease with increase of Reynolds number, the maximum enhancement of heat transfer takes place at Re = 7950 and P/Di 0.45 for dw/Di=0.05 and enhancement ratio = 153.93%

2- The enhancement ratio decrease as the wire pitch increase. The maximum, enhancement of heat of heat transfer take place at P/Di = 0.45 and Re = 7930 for dw/Di=0.07 and enhancement ratio reaches to 204.36%.

3- As the wire diameter increases the enhancement ratio increases and the maximum enhancement take place at dw/Di=0.068 and Re=7930 for P/Di=0.45 and the enhancement ratio=204.36%.

4- As the diameter ratio increase, the enhancement ratio decrease.

5- The friction ratio increases with increase of Reynolds number, the maximum friction factor ratio take place at Re=24350 and P/Di=0.45, and the friction ratio=446.33%.

6- As the wire pitch increases, the friction factor ratio decreases and the maximum friction factor ratio take place at Re=24350 and P/Di=0.4, and the friction factor ratio=451.24%.

7- The friction factor ratio increases with increasing helical wire diameter, the friction factor ratio take place at dw/Di=0.068 and Re=28920 and reaches to 462.6%.

8- The friction factor ratio increase with increasing radius ratio and the Max value 586.88% at Re = 24450 and D0/Di= 3.27 at P/Di = 0.45 and dw/Di= 0.068.

REFERENCES

1. Bharadwaj,P., Khondge, A., and Date,A., "Heat Transfer and Pressure Drop in a Spirally Grooved Tube Twisted Tape Insert", Int. Journal of Heat and Mass Transfer, Vol.52, pp. 1938-1944, 2009.
2. Raviguruajan, T.S., "A Comparative Study of Thermal Design Correlations for Turbulent Flow in Helical- Enhanced Tubes", Heat Transfer Engineering, Vol.20, pp.54-70, 1999.
3. Dewan, Mahanta, Sumithra, R., and Suresh, K., "Review of Passive Heat Transfer Augmentation Techniques", Department of Mechanical Engineering, Indian Institute of Technology, Guwahati, India.
4. Lieke, W., and Bengt, S., "Performance comparison of some Tube Inserts" Int. Comm. Heat Mass Transfer, Vol.29, pp. 45-56, 2002
5. Sivashanmugam, P. and suresh, S., "Experimental Studies on Heat Transfer and Friction Factor Characteristics of Turbulent Flow Through a Circular Tube Fitted with Regularly Spaced Helical Screw-Tape Inserts", Applied Thermal Engineering Vol.27, pp.1311-1319, Dutta, A 2007.
6. Smith, E. and Pongjet, P., "Heat Transfer Characteristics in a Tube Fitted with Helical Screw-Tape with/without Core-rod Inserts", Int. Communications in Heat and Mass Transfer, Vol.34, pp.176-185, 2007.
7. Akhavan, M.A.K., Mohsen, S.G., Najafi, H. and Ramazanzadeh, H., "Heat Transfer and Pressure Drop Characteristics of Forced Convective Evaporation in Horizontal Tubes with Coiled Wire Inserts", Int. Communications in Heat and Mass Transfer, pp. 1-7, 2009.
8. Ebru, K.A., "Evaluation of Heat Transfer and Loss in a Concentric Double Pipe Exchanger Equipped with Helical Wires", Energy Conversion and Management, Vol.47, pp.3473-3486, 2006.
9. Garimella, S., and Christensen, R.N., "Heat Transfer and Pressure Drop Characteristics of Spirally Fluted Annuli: Part I, Hydrodynamics",. ASME Journal of Heat transfer, Vol. 117, pp54-60, 1995.
10. Garimella, S., and Christensen, R.W., "Heat Transfer and Pressure Drop Characteristics of Spirally Fluted Annuli: Part II, Heat transfer ", ASME Journal of Heat Transfer, Vol. 117, PP.61-68, 1996.
11. Alberto, G., Pedro, G.V., and Antonio, V., "Heat Transfer and Pressure Drop for Low Reynolds Turbulent Flow in Helically Dimpled Tubes" Int. J. of Heat and Mass Transfer, Vol. 45, pp. 543-553, 2002.
12. Alberto, G., Pedro, G.V., and Antonio, V., "Experimental Study of Heat Transfer Enhancement with Wire Coil Inserts in Laminar-Transition-Turbulent Regimes at

Different Prandtl Numbers", Int J. Heat and Mass Transfer, Vol.48, pp.4640-4651, 2005.
13. Promvonge, P. and Eiamsa, S., "Heat transfer in a circular tube fitted with free-spacing snail entry and conical-nozzle turbulators", Int. J. Heat and Mass Transfer, vol.34,PP.838-848,2007.
14. Eiamsa, S., A. and Promvonge, P., "Heat Transfer Enhancement in a Tube with Combined Conical-nozzle Inserts and Swirl Generator", Energy conversion and Management, Vol.47, pp.2867-2882, 2006.
15. Promvonge, P. and Eiamsa, S., A., "Experimental Investigation of Heat Transfer and Friction Characteristics in a Circular Tube Fitted with V-nozzle Turbulators "Int. Communications in Heat and Mass Transfer, Vol.33, pp.591-600, 2006.
16. Saha, S.K., Dutta, A. and Dhai. S.K., "Friction and Heat Transfer Characteristics of Laminar Swirl Flow Through a Circular Tube Fitted with Regularly Spaced Twisted-Tape Elements", Int. J. Heat and Mass Transfer, Vol. 44, pp. 4211-4223, 2001.
17. Dutta, A. and Saha, S. K., "Thermohydraulic Study of Laminar Swirl Flow Through a Circular Tube Fitted with Twisted Tapes.", ASME Journal of Heat Transfer, Vol. 123, pp. 417-427, 2001.
18. Shou, S.H., Ming, H.L. and Huang, H.T., " Turbulent Heat Transfer and Flow Characteristics in a Horizontal Circular Tube with Strip-type Inserts. Part II. Heat transfer" Int. J. of Heat and Mass Transfer, Vol. 46, pp. 837-849, 2003.
19. Garcia, A., Solano, J.P., Vicente, P.G. and Viedma, A., "Flow Pattern Assessment in Tubes with Wire Coil Inserts in Laminar and Transition Regimes", Int. J. of Heat and Fluid Flow, Vol.28, pp.516-525, 2007.
20. Leonard, D.T., Bock, C.P., Byung, J.B. and Dong, H.L., "A Study on Heat Transfer Enhancement Using Straight and Twisted Internal Fin Inserts", Int., Communications in Heat and Mass Transfer, Vol.33, pp.719-726, 2006.
21. Abdel-Moneim, S.A., "Heat Transfer To Air in Turbulent Pipe Flow With Suspended Solid Powder", Msc. Thesis, Faculty of Eng., Cairo University, 1989.
22. Incoropera, F.P. and Dewitt, D.P., "Fundamentals of Heat and Mass Transfer", 3rd ed., John Wiley & Sons, New York, 1990.
23. Schlichting, H., "Boundary Layer Theory", 7th ed., McGrew- Hill,New York, 1979.
24. Liao, Q. and Xin, M.D., "Augmentation of Convective Heat Transfer Inside Tubes with Three- Dimensional Internal Extended and Twisted-Tape Inserts", Chemical Engineering Journal, Vol.78, pp.95-105, 2000.

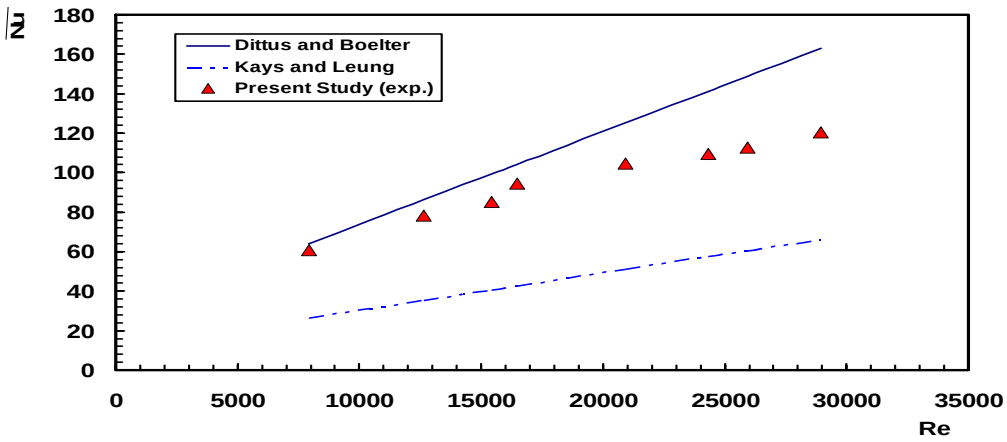

Fig.(2): Comparison between the results of the average Nusselt number vs. Reynolds number and published results.

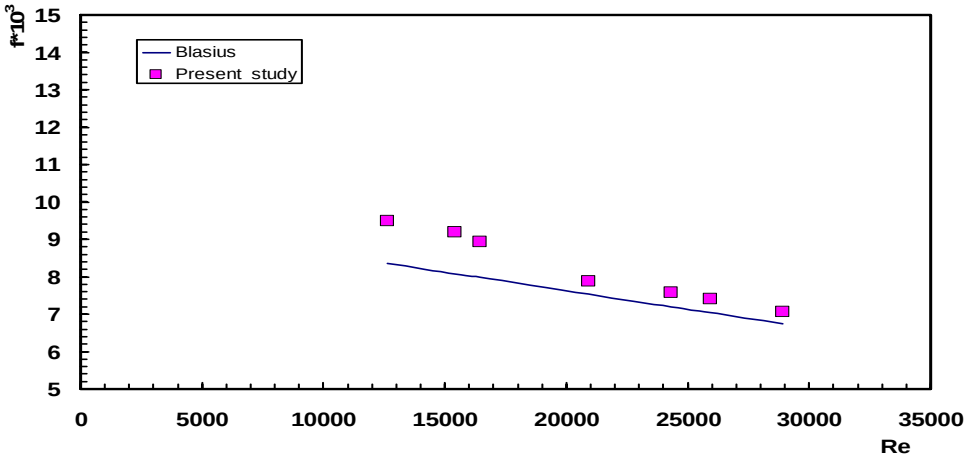

Fig.(3): Comparison between the present results of the friction factor vs. Reynolds number

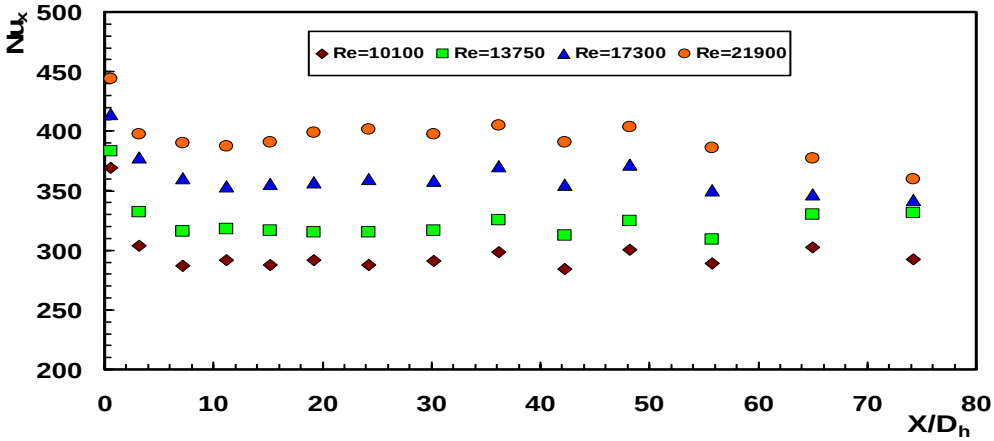

Fig.(4): Local Nusselt number for different value of Reynolds number at P/Di=0.91, dw/Di=0.07 and D0/Di=3.27.

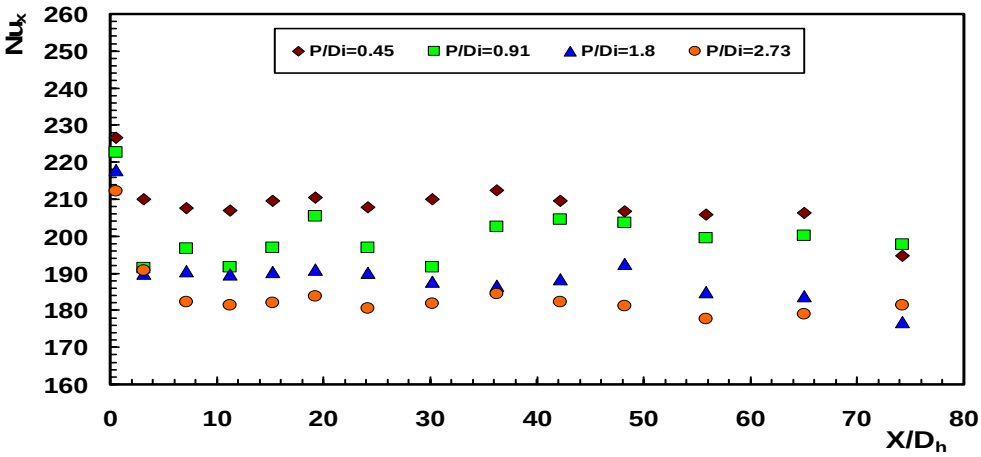

Fig.(5): Local Nusselt number for different P/Di at Re=10100, dw/Di=0.032 and D0/Di=3.27

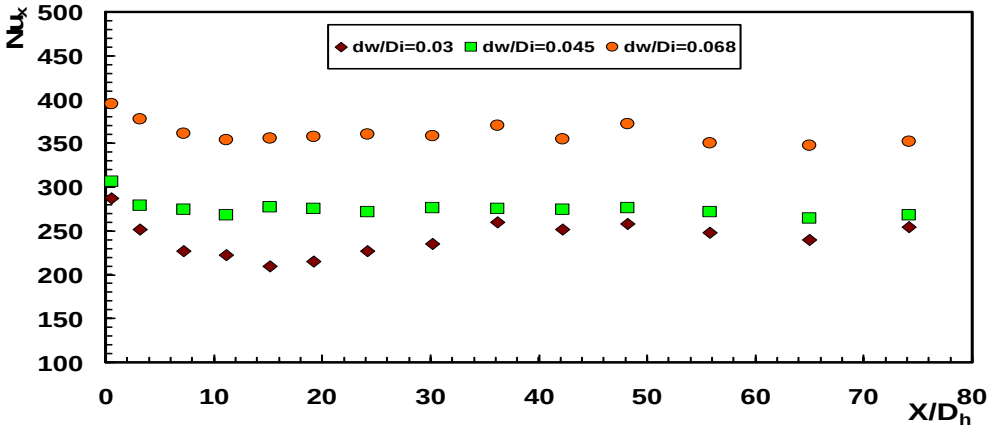

Fig.(6): Local Nusselt number for different dw/Di at P/Di=0.91, Re=17300, and D0/Di=3.27

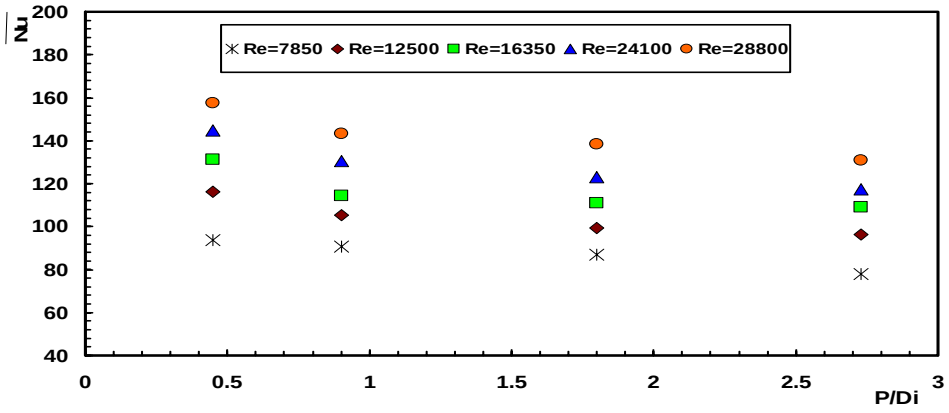

Fig.(7): The average Nusselt number versus P/Di for smooth and rough annulus at dw/Di= 0.045 for D0/Di = 2.14

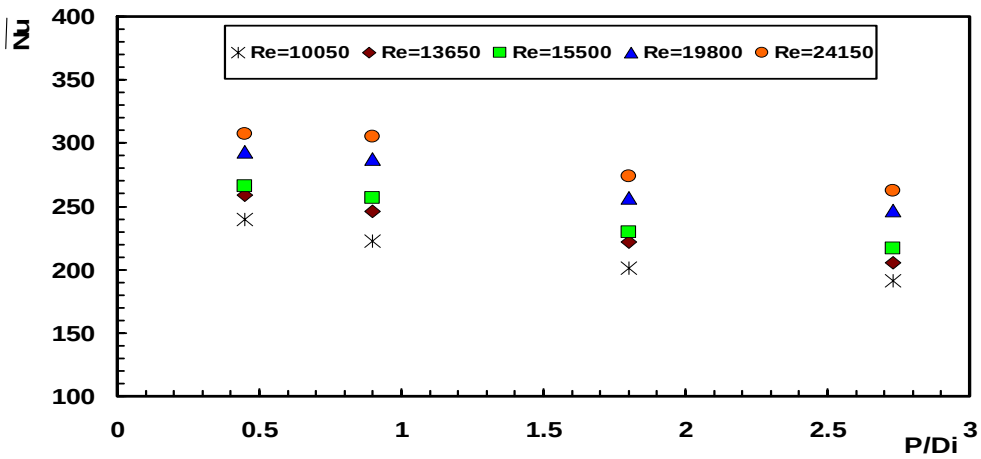

Fig.(8): The average Nusselt number versus P/Di for rough annulus at dw/Di= 0.045 for D0/Di = 3.27

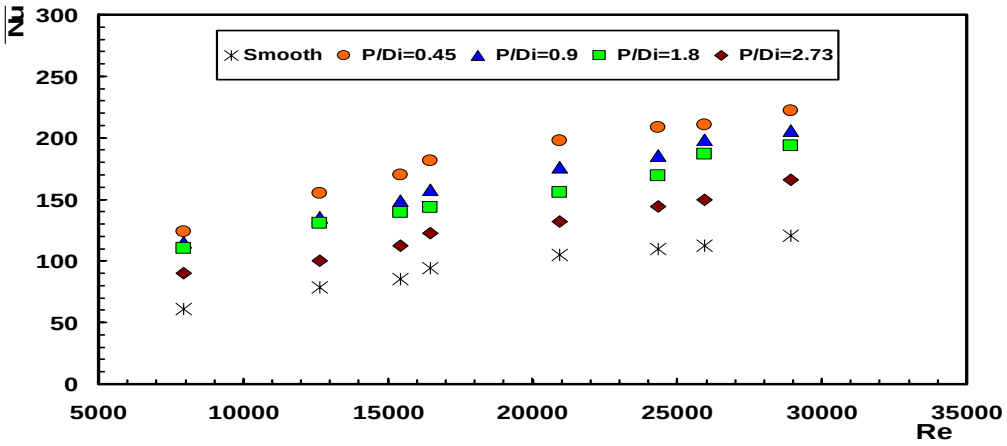

Fig.(9): The average Nusselt number versus Reynolds number for rough annulus at dw/Di= 0.068 for D0/Di = 2.14

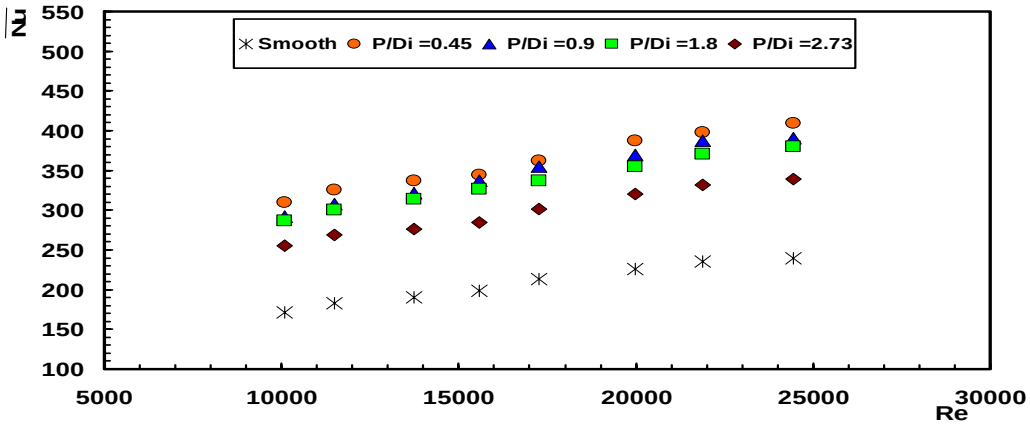

Fig.(10): The average Nusselt number versus Reynolds number for smooth and rough annulus at dw/Di= 0.068 for D0/Di = 3.27

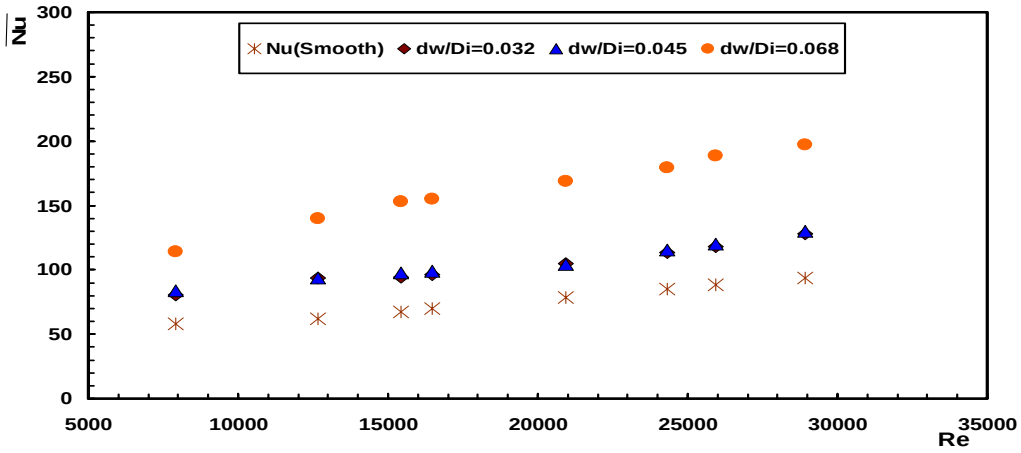

Fig.(11): The average Nusselt number versus dw/Di for smooth and rough annulus at P/Di= 0.91 for D0/Di = 2.14

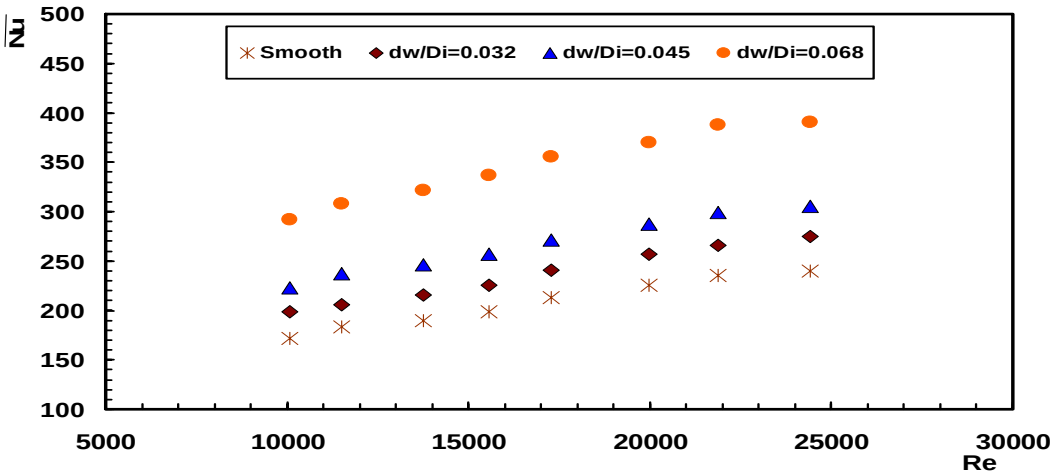

Fig.(12): The average Nusselt number versus dw/Di for smooth and rough annulus at P/Di= 0.91 for D0/Di =3.27

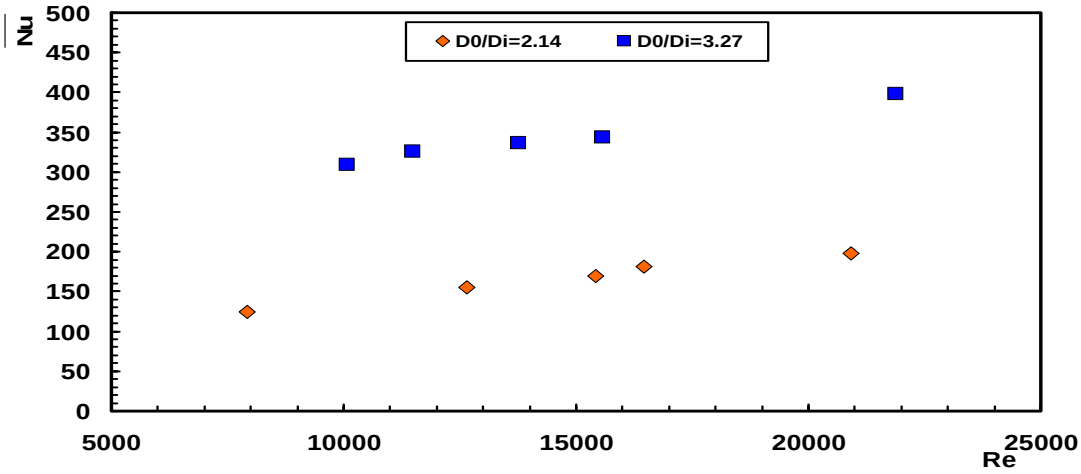

Fig.(13): The average Nusselt number versus Reynolds number for rough annulus at P/Di= 0.45, dw/Di=0.068 for different radius ratio

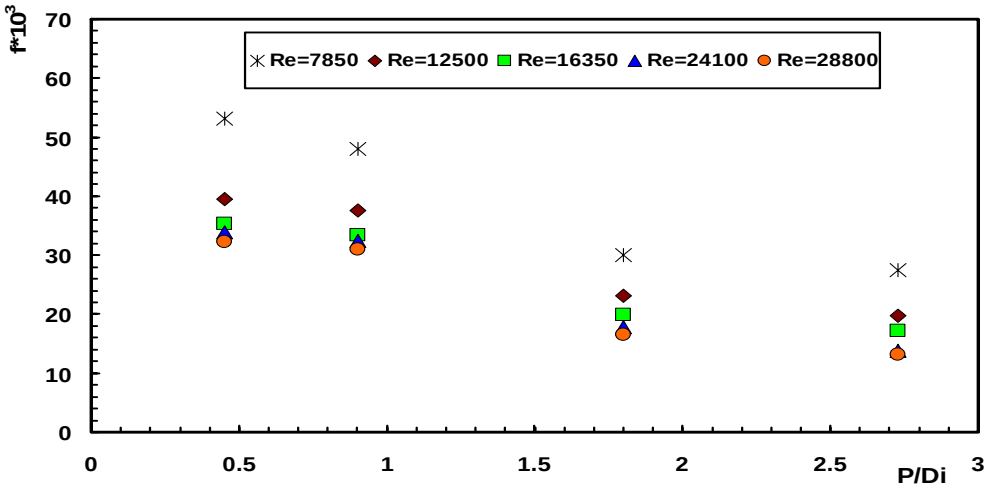

Fig.(14): The average friction factor versus P/Di for rough annulus at dw/Di= 0.045 for D0/Di = 2.14

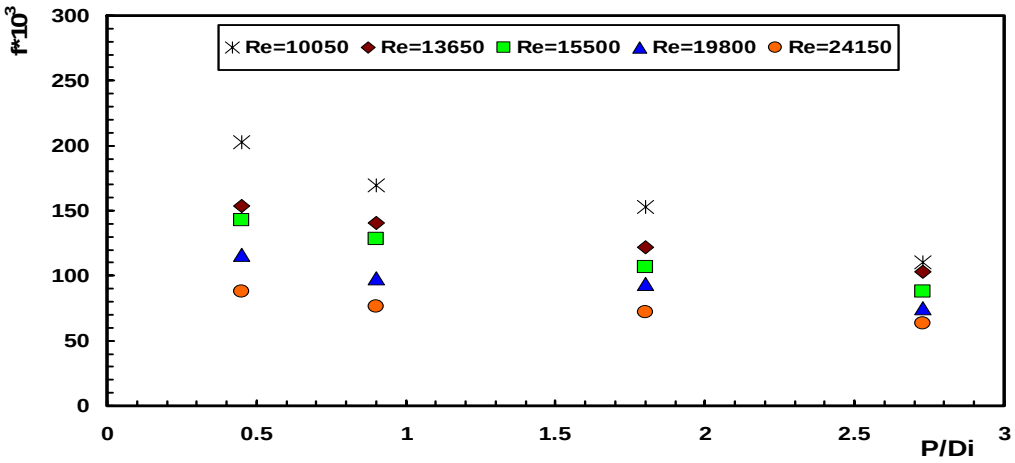

Fig.(15): The average friction factor versus P/Di for rough annulus at dw/Di= 0.045 for D0/Di = 3.27

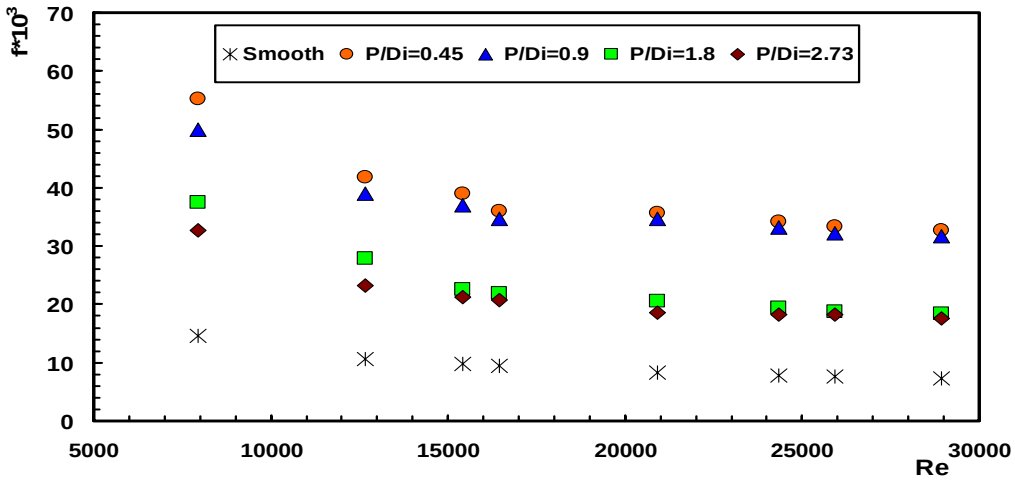

Fig.(16): The average friction factor versus Reynolds number for smooth and rough annulus at dw/Di=0.068 for D0/Di= 2.14

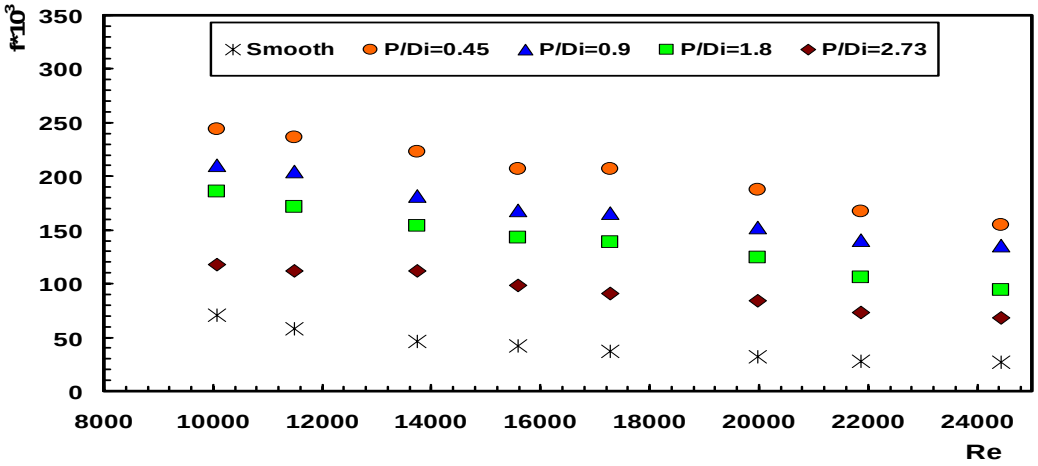

Fig.(17): The average friction factor versus Reynolds number for smooth and rough annulus at dw/Di=0.068 for D0/Di= 3.27

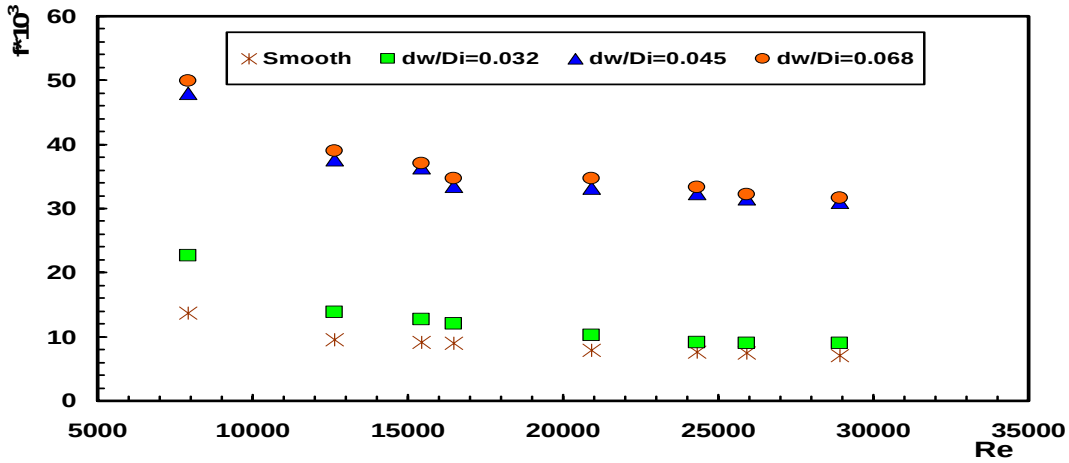

Fig.(18): The average friction factor versus dw/Di for smooth and rough annulus at P/Di= 0.91 for D0/Di =2.14

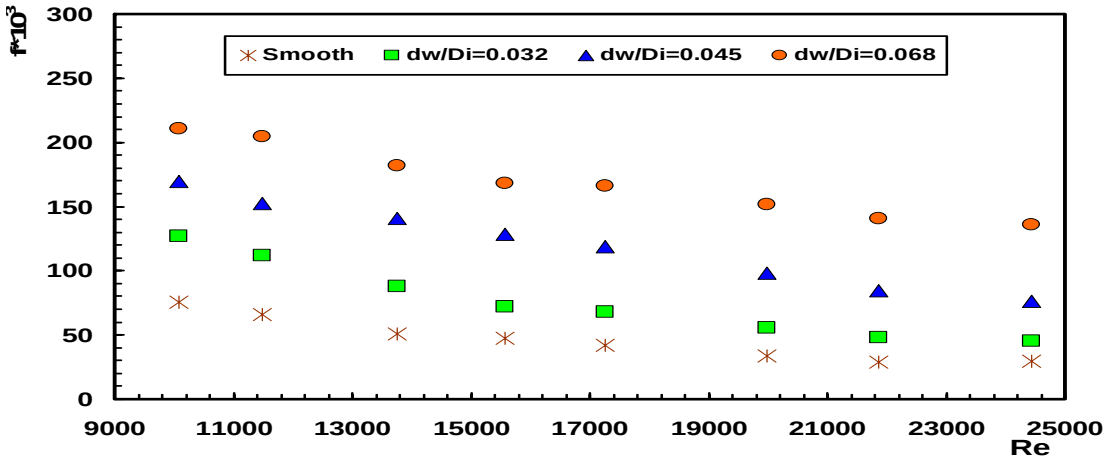

Fig.(19): The average friction factor versus dw/Di for smooth and rough annulus at P/Di = 0.91 for D0/Di =3.27

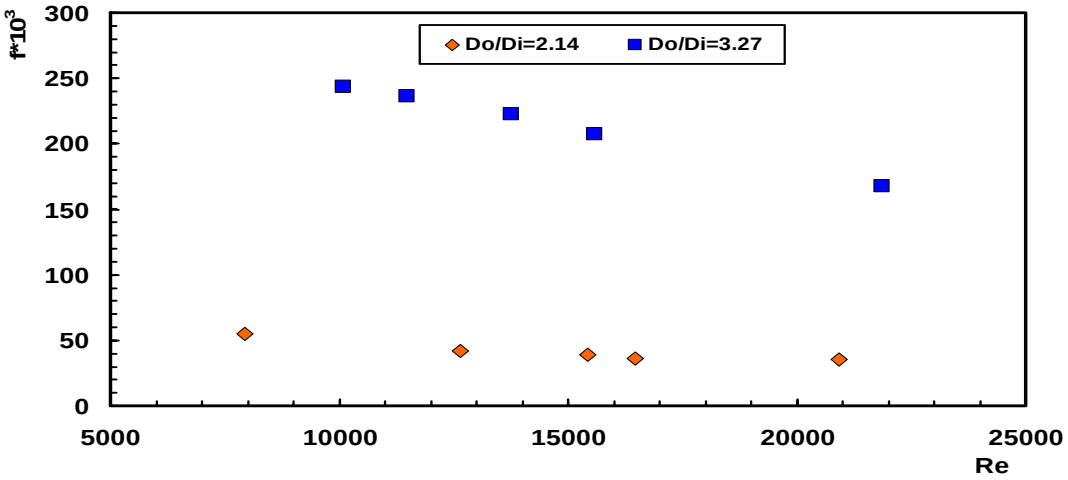

Fig.(20): The average friction factor versus Reynolds number for rough annulus at P/Di= 0.45, dw/Di=0.068 for different radius ratio

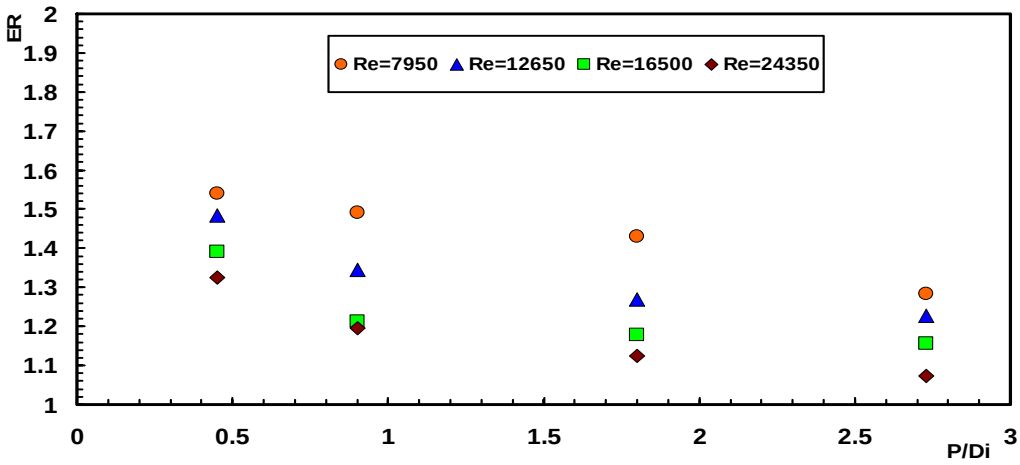

Fig.(21): Enhancement ratio versus P/Di for different Reynolds number for dw/Di=0.05 and D0/Di=2.14

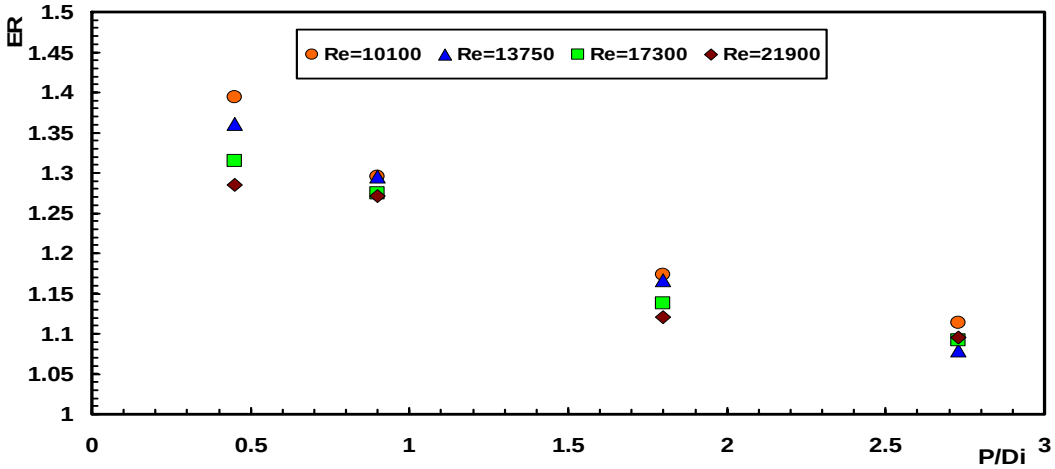

Fig.(22): Enhancement ratio versus p/d for different Reynolds number for dw/Di=0.05 and D0/Di=3.27

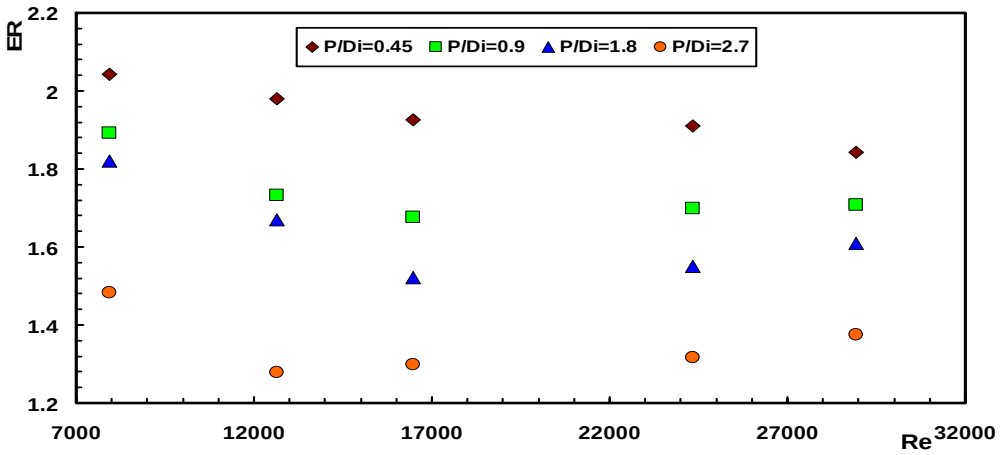

Fig.(23): Enhancement ratio versus Reynolds number for different wire pitchs (P/Di) at dw/Di=0.07 and D0/Di=2.14

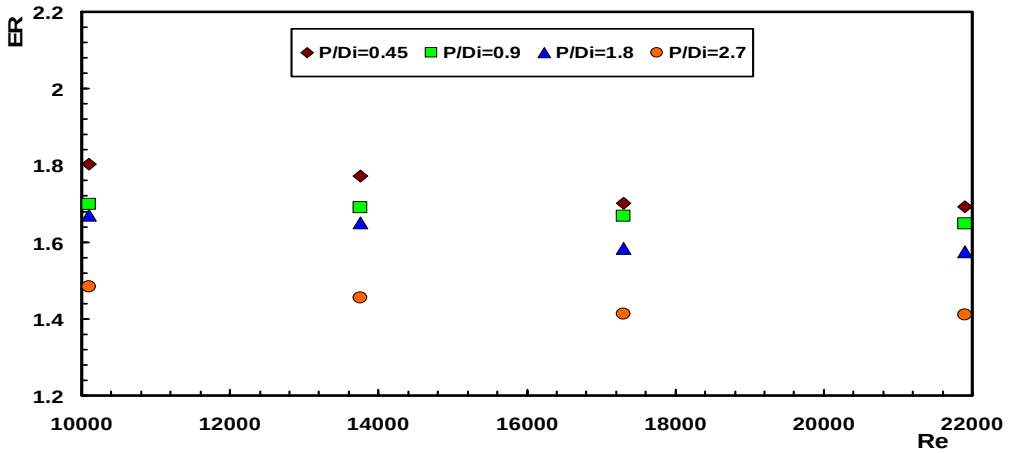

Fig.(24): Enhancement ratio versus Reynolds number for different (P/Di) at dw/Di=0.07 and D0/Di=3.27

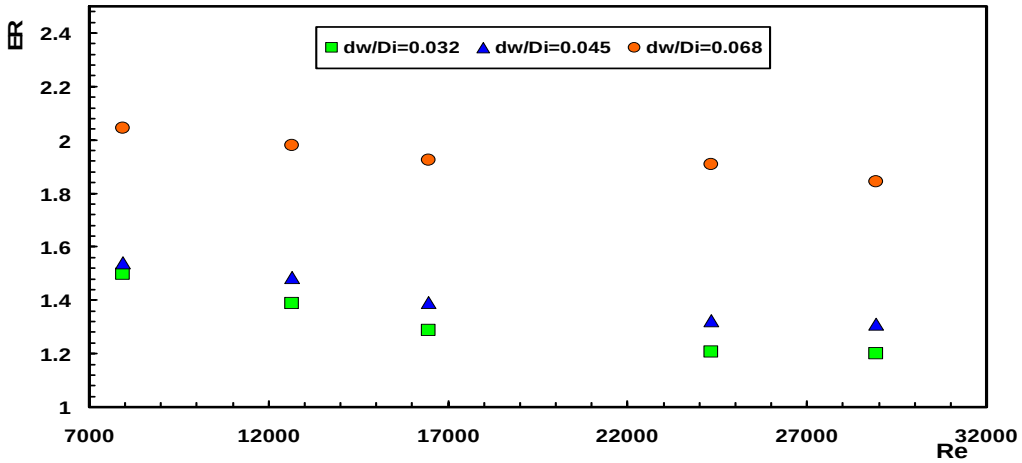

Fig.(25): Enhancement ratio versus dw/Di for different Reynolds number for P/Di=0.45 and D0/Di=2.14

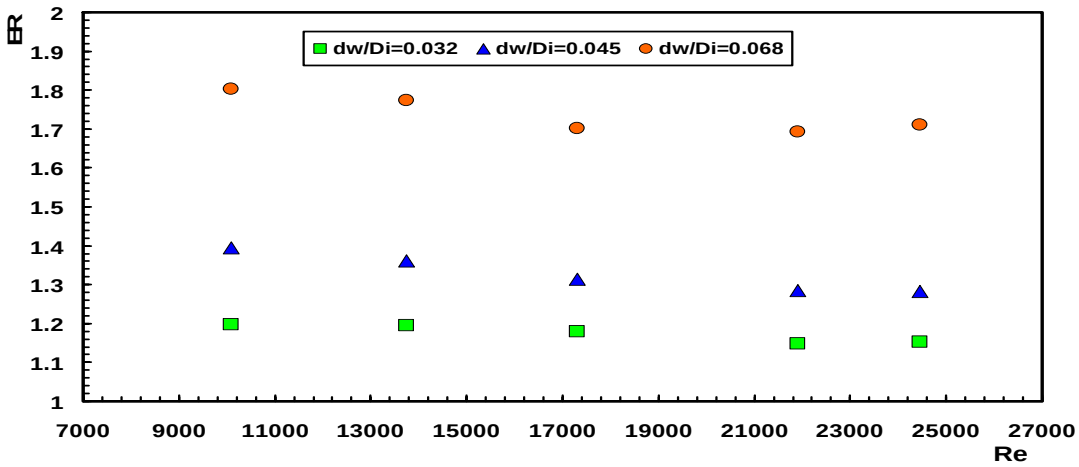

Fig.(26): Enhancement ratio versus dw/Di for different Reynolds number for P/Di=0.45 and D0/Di=3.27

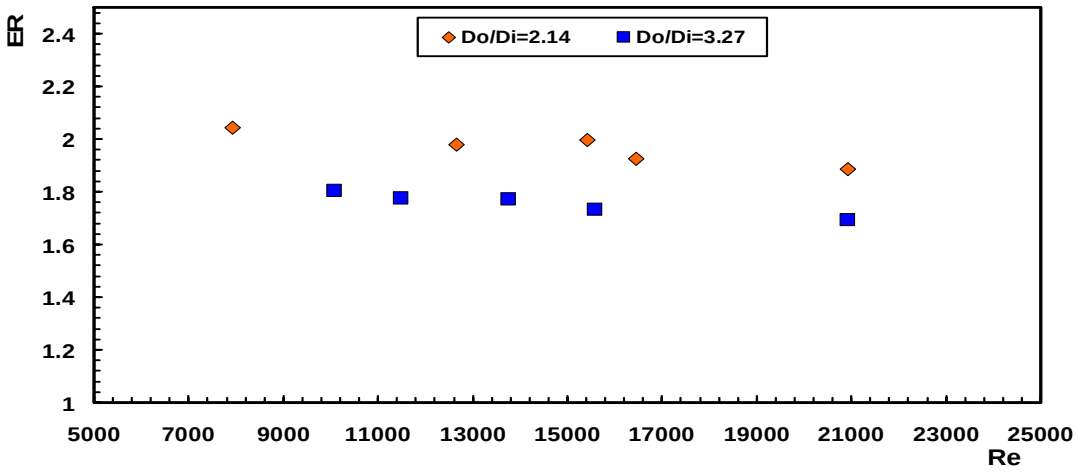

Fig.(27): Enhancement ratio versus Reynolds number for different diameter ratio at P/Di=0.45 and dw/Di=0.068

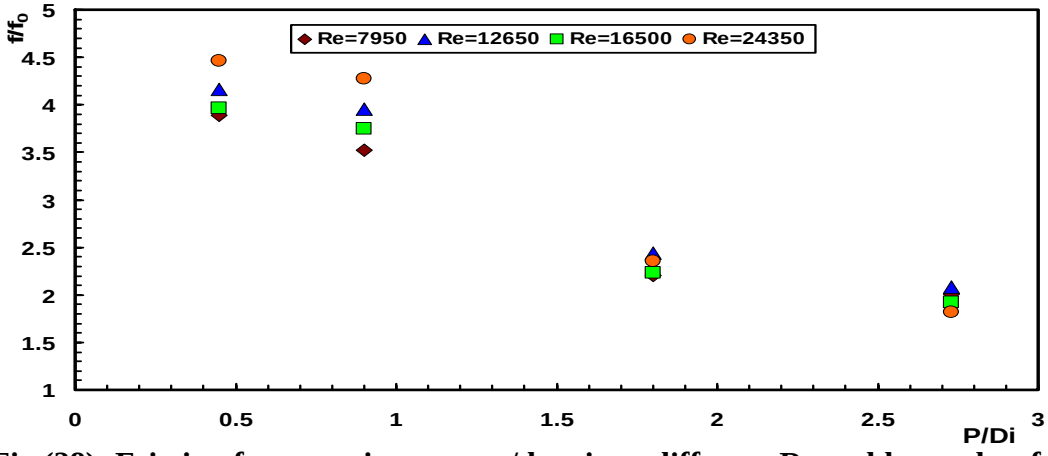

Fig.(28): Friction factor ratio versus p/d ratio at different Reynolds number for dw/Di=0.05 and D0/Di=2.14

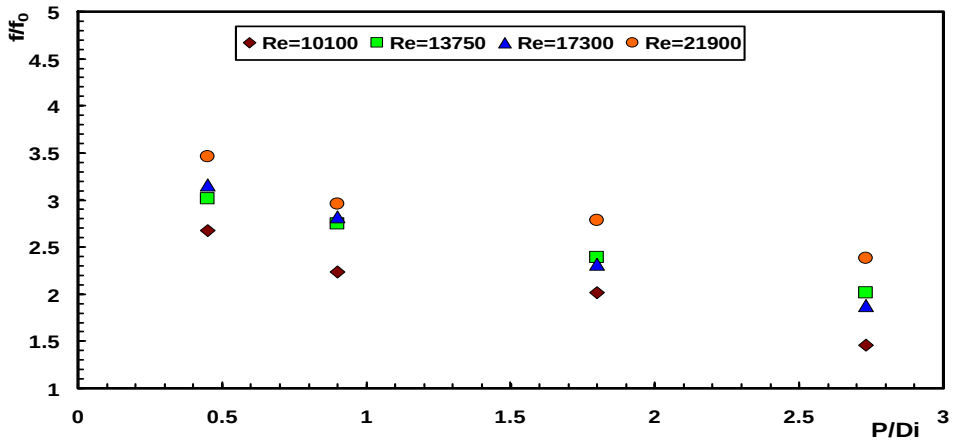

Fig.(29): Friction factor ratio versus P/Di ratio at different Reynolds number for dw/Di=0.05 and D0/Di=3.27

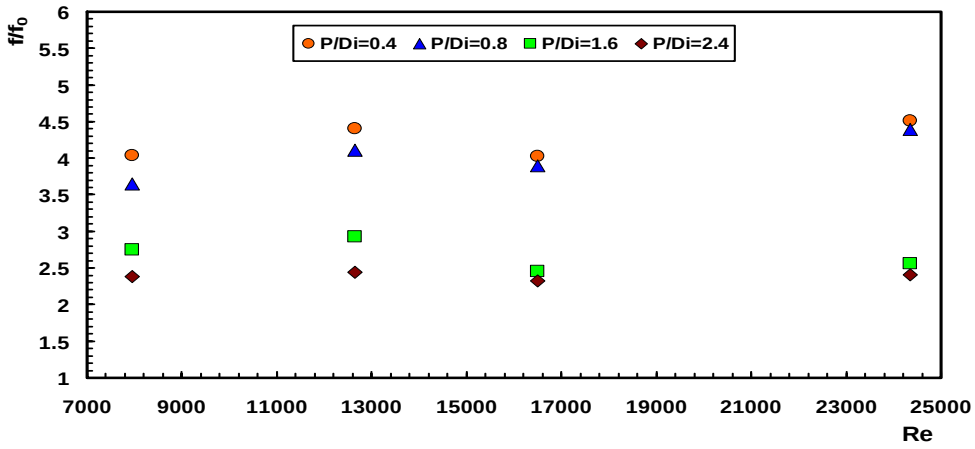

Fig.(30): Friction factor ratio versus Reynolds number for different P/Di ratio at dw/Di=0.068 and Do/Di=2.14

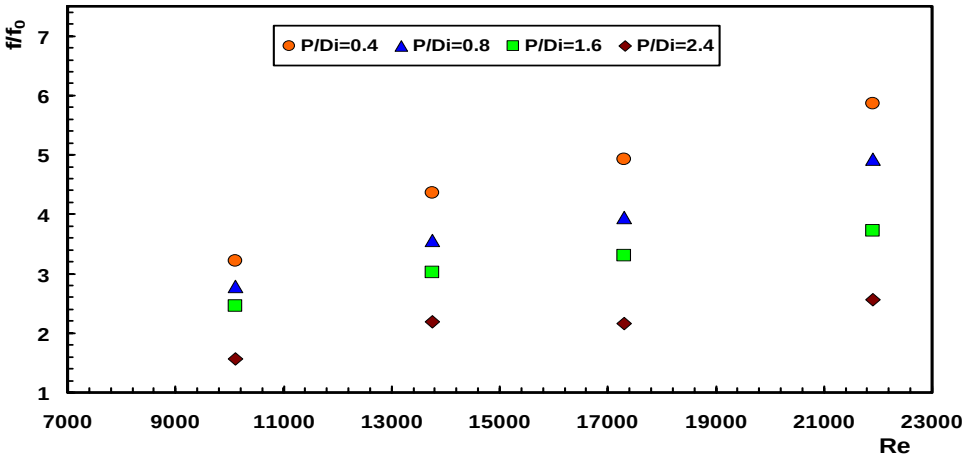

Fig.(31): Friction factor ratio versus Reynolds number for different P/Di ratio at dw/Di=0.068 and D0/Di=3.27

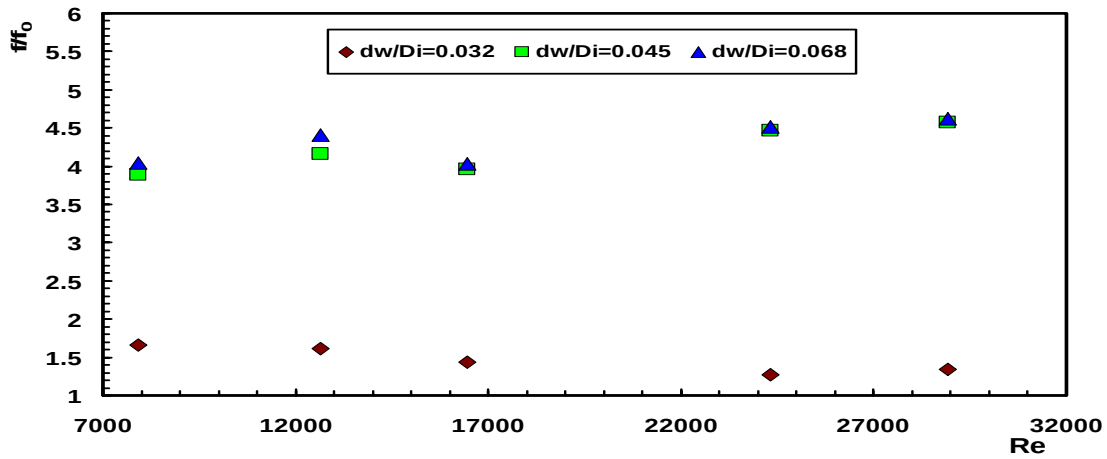

Fig.(32): Friction factor ratio versus dw/Di ratio at different Reynolds number for P/Di=0.45 and D0/Di=2.14

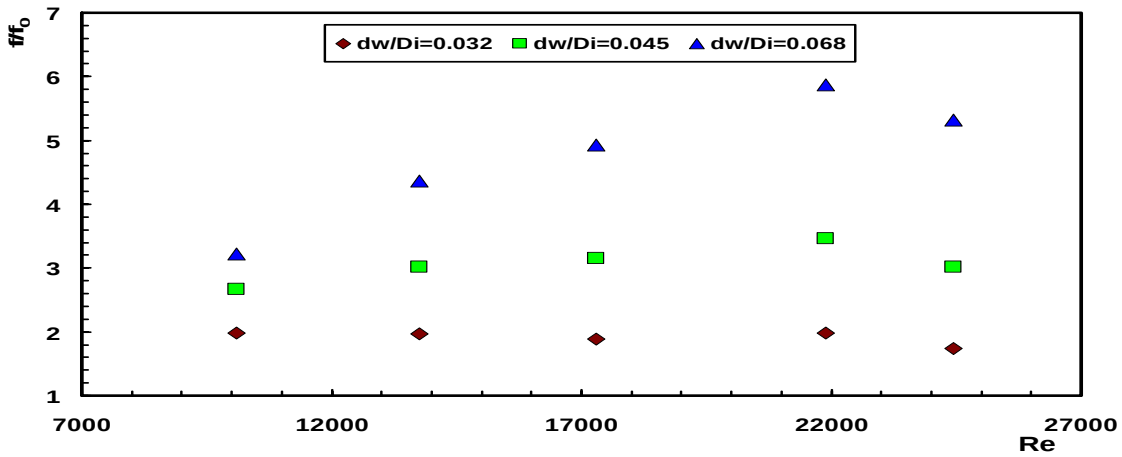

Fig.(33): Friction factor ratio versus dw/Di ratio at different Reynolds number for P/Di=0.45 and D0/Di=3.27

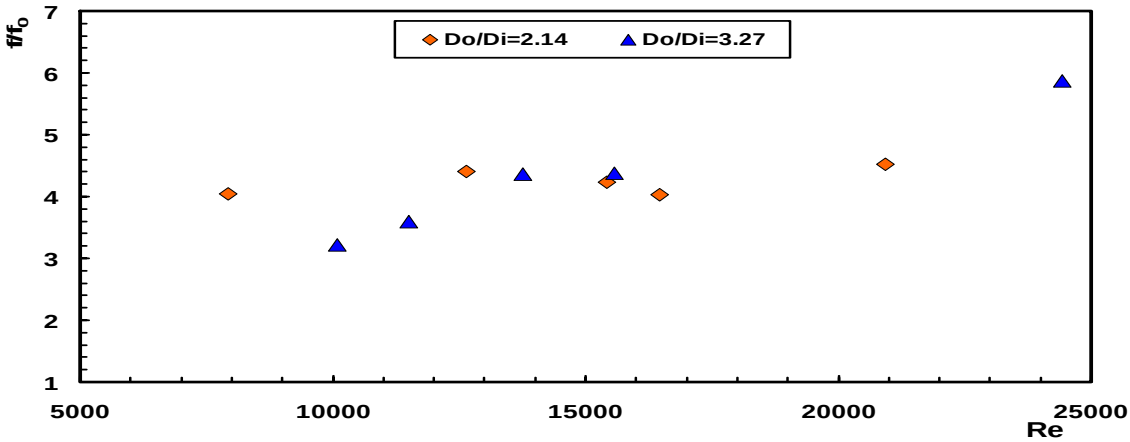

Fig.(34): Friction factor ratio versus Reynolds number for P/Di=0.45 and dw/Di=0.068 for different radius ratio

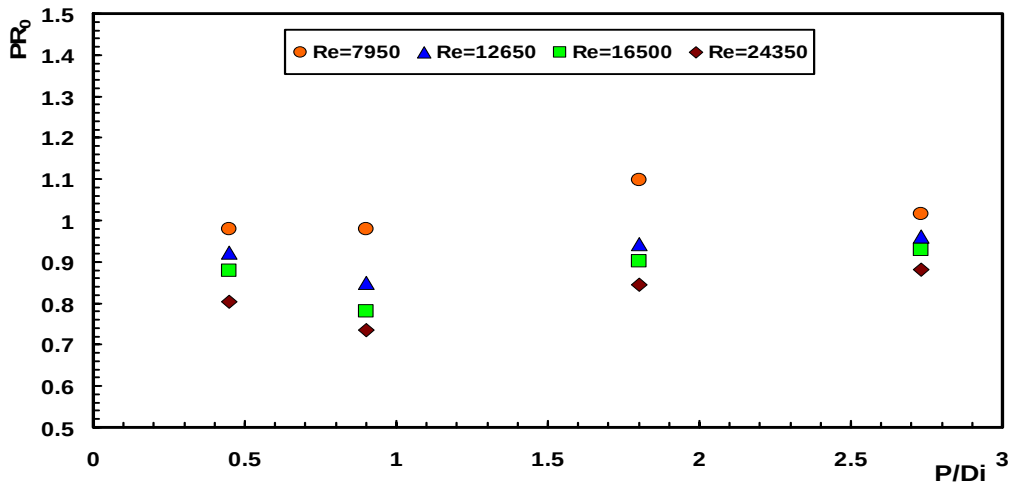

Fig.(35): The performance ratio versus Reynolds number for different P/Di at dw/Di=0.068 and D0/Di=2.14

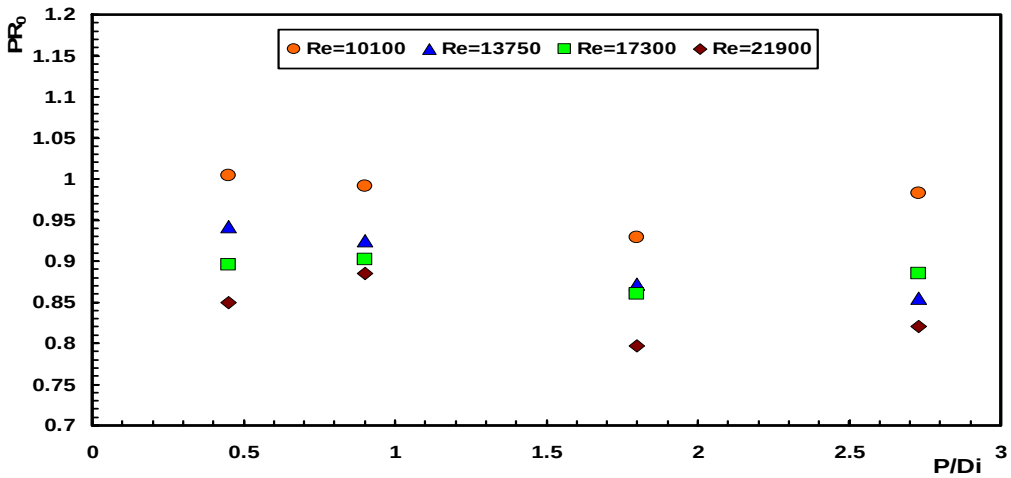

Fig.(36): The performance ratio versus Reynolds number for different P/Di at dw/Di=0.068 and D0/Di=3.27

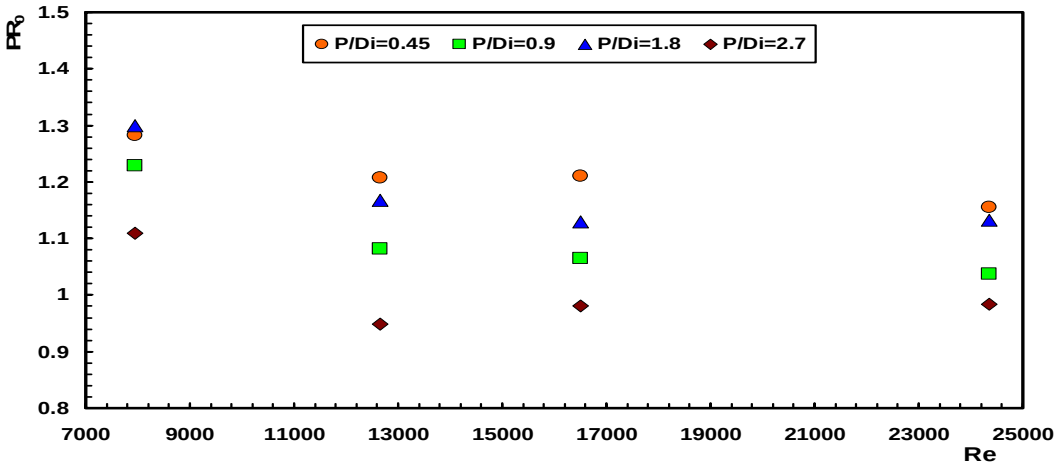

Fig.(37): The performance ratio versus P/Di for different Reynolds number at dw/Di=0.045 and Do/Di=2.14

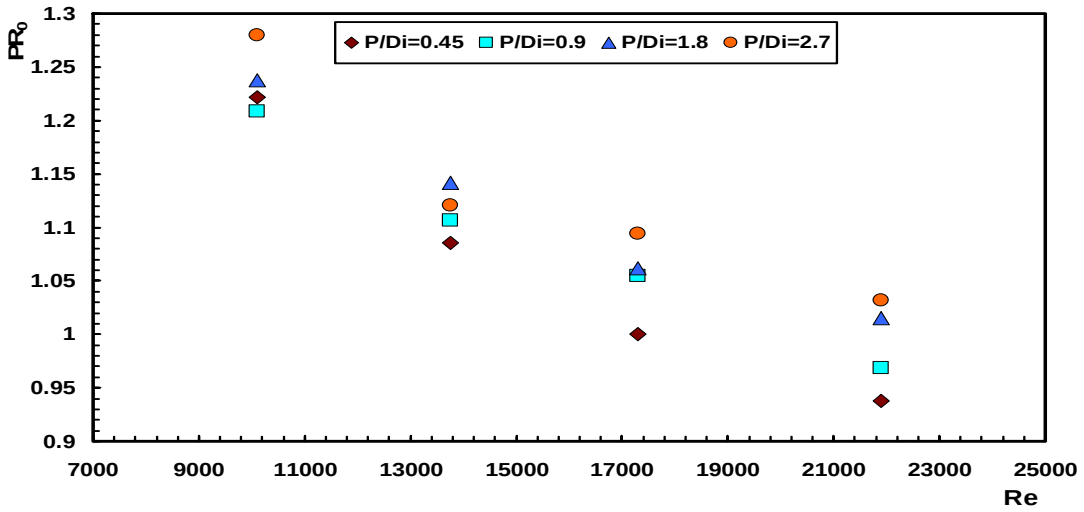

Fig.(38): The performance ratio versus P/Di for different Reynolds number at dw/Di=0.045 and D0/Di=3.27

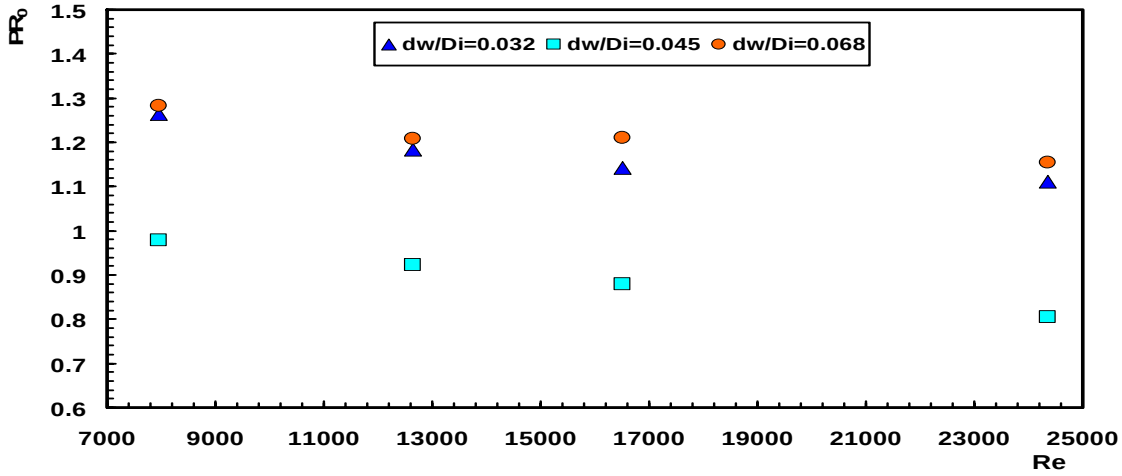

Fig.(39): The performance ratio versus dw/Di at different Reynolds number for P/Di=0. 45 and D0/Di=2.14

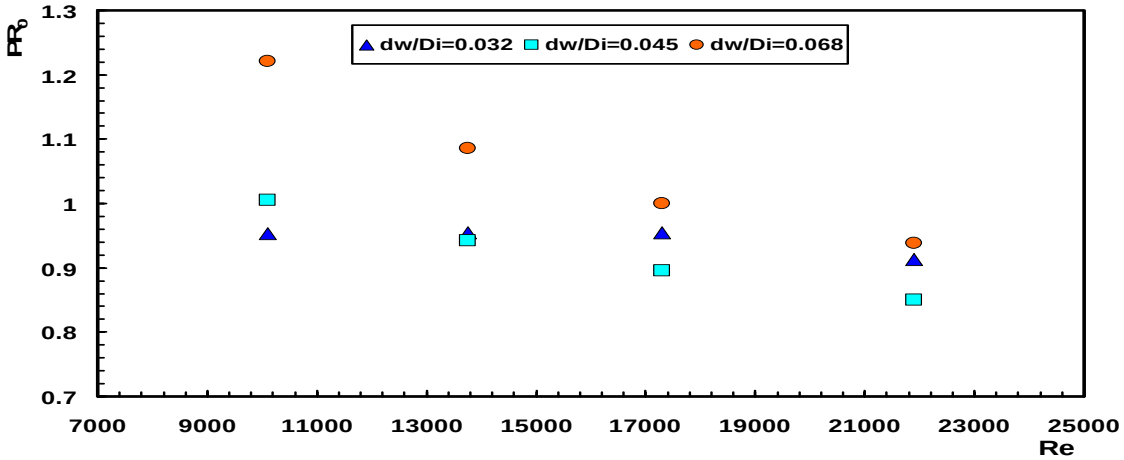

Fig.(40): The performance ratio versus dw/Di at different Reynolds number for P/Di=0. 45 and Do/Di=3.27